

Spectral indices for tracing leaf water status with hyperspectral reflectance data

Qazi Muhammad Yasir^{a,b}, Zhijie Zhang^{c,*}, Jiakui Tang^{d,e,*},
Muhammad Naveed^f, and Zahid Jahangir^g

^aUniversity of Chinese Academy of Sciences, Key Laboratory of Digital Earth Science, Aerospace Information Research Institute, Beijing, China

^bUniversity of Limerick, Mary Immaculate College, Department of Geography, Limerick, Ireland

^cThe University of Arizona, School of Geography, Development, and Environment, Tucson, Arizona, United States

^dUniversity of Chinese Academy of Sciences, College of Resources and Environment, Beijing, China

^eUniversity of Chinese Academy of Sciences, Yanshan Earth Key Zone and Surface Flux Observation and Research Station, Beijing, China

^fNortheast Normal University, Ministry of Education, School of Geographical Sciences, Key Laboratory of Geographical Processes and Ecological Security in Changbai Mountains, Changchun, China

^gWuhan University, Key Laboratory of Information Engineering in Surveying, Mapping and Remote Sensing, Wuhan, China

Abstract. Plant water stress can be detected via remote sensing. The objective of the study was to determine which leaf water index is best for assessing leaf water content from the laboratory standpoint. This study investigated the relationship between equivalent water thicknesses (EWT), gravimetric water content (GWC), and plant water concentration in the 350- to 2500-nm reflectance spectral range. A total of 277 leaf samples taken from ten different plants were used as calibration dataset, and 605 leaves from different plants, including LOPEX93 and ANGERS database, were used for validation. Three specific indices were analyzed: simple ratio, normalized ratio, and double difference (Datt type of index). A regression approach based on the iteration method at 5-nm interval was used for model calibration. Three bands index was found the most suitable and was validated by 605 leaf samples: for the linear regression model, the index is $(R_{1910} - R_{1340}) / (R_{1910} - R_{1125})$ with $R^2 = 0.96$ and root mean square error (RMSE) = 0.001 (g/cm²) and, for nonlinear regression model the index is $(R_{1930} - R_{1425}) / (R_{1930} - R_{1360})$ with $R^2 = 0.95$ and RMSE = 0.001 (g/cm²) for EWT. The newly proposed indices take advantage of being able to eliminate additional noise created by the leaf surface, making them helpful for agricultural-related research. © The Authors. Published by SPIE under a Creative Commons Attribution 4.0 International License. Distribution or reproduction of this work in whole or in part requires full attribution of the original publication, including its DOI. [DOI: [10.1117/1.JRS.17.014523](https://doi.org/10.1117/1.JRS.17.014523)]

Keywords: equivalent water thickness; plant water concentration; gravimetric water content; reflectance; remote sensing; hyperspectral indices.

Paper 220574G received Oct. 6, 2022; accepted for publication Mar. 13, 2023; published online Mar. 31, 2023.

1 Introduction

Water is the essential variable affecting crop productivity; there is a direct link between biomass output and water absorbed through transpiration.¹ In many parts of the world, water shortages brought about by climate change have forced plants to endure severe water stress, which has reduced food yield. Variability in leaf water content is important for plant–environment interactions, ecosystem function, and crop development. Photosynthesis, evapotranspiration, and net primary productivity are all affected by plant leaf water content. Estimating each plant's

*Address all correspondence to Zhijie Zhang, zhangzhijie@arizona.edu; Jiakui Tang, jktang@ucas.ac.cn

hydration status is required to schedule the irrigation times of a crop and the amount of water it requires. However, estimating water content accurately using reflectance factors across diverse plant species remains difficult.^{1,2} Global climate change and biodiversity loss significantly impact species and ecosystem functions, which in turn affects processes at the regional and landscape sizes and disturbs the world's biogeochemical cycles.³ Important factors in a range of environmental processes include the water content of leaves and the canopy.⁴

Remote sensing has gained popularity as a technology to track and measure vegetation characteristics in recent years. Plant responses to environmental factors and their impact on ecosystem processes, including adaptations to climate change, are influenced by canopy biophysical and biochemical variables involved in the biophysical processes of terrestrial ecosystems.⁵ Remote sensing technology is particularly effective in monitoring leaf water content over a large area, and it is also useful for detecting water stress, assessing fire danger, and scheduling irrigation. Water and dry matter in leaves impact near-infrared and shortwave infrared (SWIR) reflectances, which are additionally controlled by leaf structure, canopy structure, and leaf area index (LAI).⁶⁻⁸

Hyperspectral remote sensing is promising for detecting vegetation water content and can potentially reveal the whole scenario from a small to a large scale.⁹ Literature related to hyperspectral remote sensing, different wavelengths, and indices were claimed by researchers to establish a satisfying correlation with leaf water content for equivalent water thickness (EWT), plant water concentration (PWC), and gravimetric water content (GWC).^{10,11} The reliability of direct water absorption characteristics has resulted in the introduction of simple band ratio indices for assessing plant water using optical remote sensing.⁷ The first stage in developing an operational approach for retrieving vegetation water content via hyperspectral remote sensing is clearly defining and illustrating the possibilities. It is crucial to remember that, for the provided algorithm indices, the water absorption wavelengths employed vary slightly depending on the scenario to achieve the best absorption bands.^{12,13}

Numerous algorithms to extract leaf water content from spectral data have been described in light of the design that the depth and shape of the water-related absorption band are indicative of the water content of leaves. Studies show slightly varied ideal absorption bands, even if the water-absorption wavelengths employed in the algorithms indices are not necessarily the same.^{14,15} When evaluating the likelihood of wildfires or determining the drought status in forestry and agriculture, it is crucial to understand how the earth's ecosystems function. For instance, the water content of vegetation restricts biochemical processes, such as photosynthesis and evaporation.^{5,15}

Many methods for estimating leaf water content from reflectance data at different levels have been developed; however, they generally rely on empirical or physical approaches that use regression techniques using hyperspectral indices and leaf and canopy radiative transfer models.^{16,17} Ordinary least squares regression approaches are often used at the leaf level to build empirical correlations between leaf water content and laboratory reflectance data acquired in the near- and short-infrared spectral regions. Using acceptable spectral reflectance indices, several investigations have employed empirical relationships to assess leaf water content.¹⁸

A fast, accurate, and non-destructive means of determining the status of the water is provided by remote sensing techniques. Spectral reflectance measurements have been connected to several markers of water quality.^{19,20} Investigations at the leaf level showed that the assessment of leaf water content in terms of EWT expressed in the quantity of water per unit area (g/cm^2) was more accurate than moisture content expressed in the quantity of water per quantity of fresh or dry mass.^{12,21,22}

The visible and near-infrared region (0.4 to $2.50 \mu\text{m}$) may be divided into seven primary sections based on varied features of green plant leaves.²³ The three most relevant bands for the remote sensing of green vegetation are chlorophyll absorption band, highly reflective leaf structure band, and broad foliar water absorption band, which stretch from 0.63 to $0.69 \mu\text{m}$, 0.74 to $1.10 \mu\text{m}$, and 1.35 to $2.50 \mu\text{m}$, respectively.^{24,25} In SWIR, specifically at 1450 , 1940 , and 2500 nm wavelength, strong water absorption can be detected, whereas in the NIR region close to 970 - and 1200 -nm wavelength, the water absorption is very weak. Therefore, remote sensing techniques can be used to assess vegetation water content from radiation reflected from leaves and canopies.

The EWT is extremely important in various processes, including photosynthesis, evaporation, and primary conductivity,²⁶ and is closely correlated with the depth of SWIR absorption bands; hence, it has a higher link with spectral leaf features.¹¹ It takes time and involves productivity errors to measure leaf water content precisely and accurately. Because laboratory research also enables us to identify the many wavelengths where water content has a significant impact on leaf reflectance factor.²⁷

Gravimetric measurement is sometimes regarded as the most used destructive approach because of its excellent dependability and simplicity. The GWC, defined as the ratio of leaf water mass to leaf dry or fresh mass and given as a percentage, is a popular way to quantify leaf water content.²⁸ The vegetation fuel community prefers the GWC in dry mass form, but the ecological community prefers it in fresh mass form. The optical domain determination of GWC was based on the link between reflectance at 700 to 2500 nm and the amount of water present.^{23,29} The spectral variation induced by changes in leaf GWC is related to changes in both leaf water absorption and dry matter absorption.¹² Dry matter absorbs light in the SWIR band, which is unfortunately hidden by the presence of water in young leaves.¹⁸

The PWC measurements are important for irrigation techniques and natural community drought assessments. The usual method for measuring water concentration, which involves drying plant leaves in an oven, is straightforward and dependable, but it is also time-consuming and labor-intensive. It has been demonstrated that utilizing electromagnetic and infrared radiation to absorb water is a viable technique for determining plant water contents.^{15,20}

Plant development is dependent on the availability of water.³⁰ The leaf scale water content is one of the most important physiological measures for determining plant water status among all known physiological parameters.²⁵ Unfortunately, our understanding is severely limited by the availability of reliable field sampling/monitoring data on plant water status and plant water use until the present, which is far beyond the requirement for assessing the impacts of global change.³¹

Comparatively, plant water use (transpiration) has been far less investigated through hyperspectral reflectance. Developed approaches of hyperspectral remote sensing for retrieving plant traits can typically be grouped into two categories: physically based inversions and empirically/statistically based methods. Both approaches widely retrieve biophysical and biochemical variables from hyperspectral information.³²

Remote sensing has been used widely for detecting water stress at the leaf, canopy, and forest scales in terms of EWT, GWC, and PWC.³³ Variability in leaf water content influences plant-environment interactions and crop development.³⁴

This research is mostly concerned with:

- 1) to evaluate the performances of different published indices with our study site data.
- 2) To find out the relationship between the reflections of leaves and plant water content.
- 3) To determine the new remote sensing index for leaf water content estimation.

The study's findings will assist in identifying, calculating, and clarifying the problems raised above. It will also assist in segmenting plant species to allow efficient and successful precision agriculture.

2 Material and Methods

2.1 Leaf Sampling in the Study Area

Leaves from ten unique plants, including *Prunus padus* L., *Swida alba* Opiz, *Acer saccharum* Marsh, *Armeniaca vulgaris* Lam., *Populus* L., *Epipremnum aureum*, *Schefflera microphylla* Merr, *Pachira aquatica*, *Juglans*, and *Citrus limon* (L.) Burm. F. were collected from the Garden of Northeast Normal University, Changchun, Jilin, China. A total of 277 samples of 10 unique plant species were collected, as shown in Fig. 1. The basic statistics for the calibration dataset is shown in Table 2. All samples were collected by the most reliable and accurate method for reflectance. Before measurement, the samples were kept hydrated in a dark environment with high humidity and a low temperature, and all of the samples were mature leaves.^{35–38} As in other studies, we only selected fresh leaves with a consistent color with no obvious signs of illness.^{39,40}

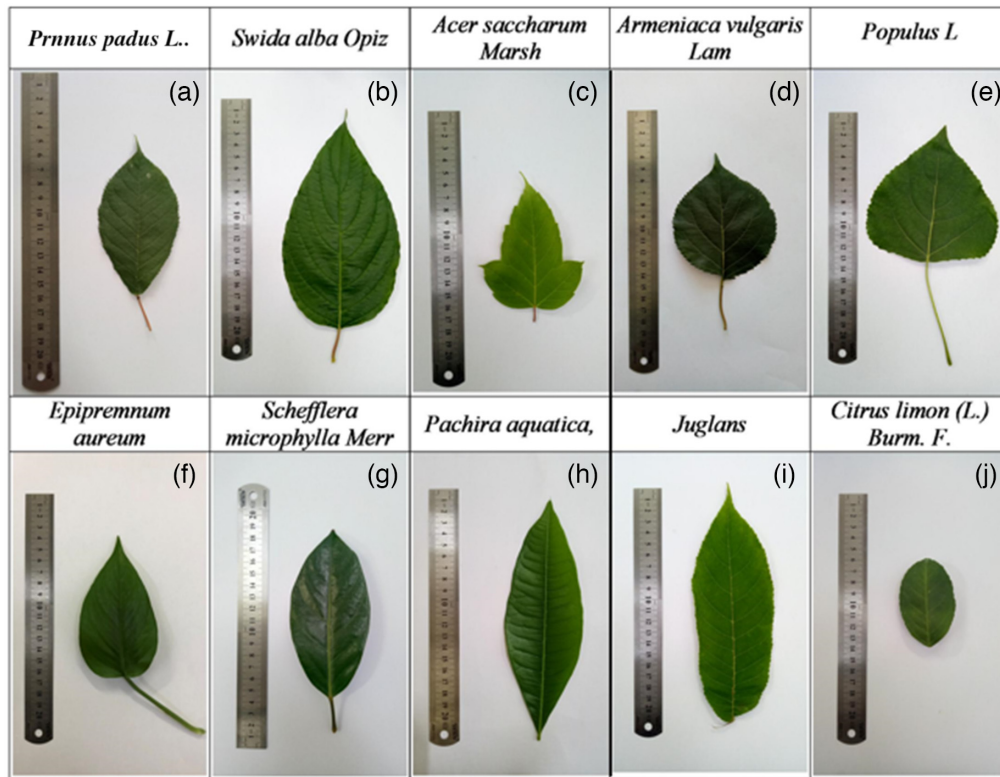


Fig. 1 (a)–(j) Leaf samples from various plant types were used in this research.

To detect spectrum reflection, we utilized the Northeast Normal University Laboratory Goniospectrometer System (NENULGS).⁴¹ An Analytical Spectral Devices FieldSpec4 and a goniometer was included in NENULGS, which was comprehensively discussed in the article.⁴¹ Several research studies have used NENULGS to analyze various leaf characteristics^{42–44} precisely. The reflectance measurement was followed by a fresh weight measurement, which was afterward air-dried to a stable weight. The samples were dried in the oven for 36 hrs at 80°C, and their dry weight was calculated.³⁸ While the measurements were being taken, the leaf sample was placed on an object stage entirely covered with dark black tape. Because the black backdrop has a wavelength-independent reflectance factor of less than 0.05, it does not affect leaf reflection. The reflected radiance (dL_{Sample}) from the leaf sample surface is normalized by the reflected radiance ($dL_{\text{Reference}}$) from the reference surface (Spectralon) in the same viewing geometry to give the bidirectional reflectance factor (BRF)⁴⁵

$$\text{BRF}(\lambda, \theta_s, \theta_v, \varphi_s, \varphi_v) = \frac{dL_{\text{Sample}}(\lambda, \theta_s, \theta_v; \varphi_s, \varphi_v)}{dL_{\text{Reference}}(\lambda, \theta_s, \theta_v; \varphi_s, \varphi_v)} \rho_\lambda. \quad (1)$$

2.2 Definition of Water Equation Used

Several techniques, which include EWT, PWC, and GWC, were used to assess the water condition of leaves. EWT is the term used to describe how much water is present and how much energy is absorbed per unit of leaf area.^{28,46} PWC relates to the dry weight ratio, and GWC determines the weight of the fresh and dry leaves.

Below is the correspondence for EWT, PWC, and GWC

$$\text{EWT} (\text{g}/\text{cm}^2) = \frac{(W_F - W_D)}{\text{LA}}, \quad (2)$$

$$PWC = ((W_F - W_D)/W_D)100, \tag{3}$$

$$GWC_F = \frac{(W_F - W_D)}{W_F}, \tag{4}$$

and

$$GWC_D = (W_F - W_D)/W_D, \tag{5}$$

where W_F , W_D , and LA refer to fresh weight, dry weight, and leaf area, respectively.

2.3 Choosing the Optimal Index by Iteration Method

We implemented the Datt type of index (combination of three different bands), which has been popularly used recently.⁴⁷ For EWT, PWC, and GWC, using MATLAB code to assess the best index in this study using a 5-nm wavelength interval with iteration method on the calibration datasets. The iteration process was programmed in such a way that those wavelength combinations with higher R^2 come out from the large amount of data, which has been taken during leaf sample reflection measurement. The equation is defined as

$$Datt = (R_{\lambda1} - R_{\lambda2})/(R_{\lambda1} - R_{\lambda3}), \tag{6}$$

where $R_{\lambda1}$, $R_{\lambda2}$, and $R_{\lambda3}$ represent radiance at certain wavelengths (250 to 2500 nm) at $\lambda1$, $\lambda2$, and $\lambda3$, correspondingly.

2.4 Published leaf Water Indices

Different hyperspectral indices depend on the double difference ratio of three individual wavelengths within a specific spectrum and have been taken into account to figure out plant water content on the calibration dataset. For this analysis, ten previously published indices were chosen to test their effectiveness regarding how they respond to the data from the leaf dehydration experiment used in this work. The selected indices are listed in Table 1.

Table 1 Published water indices for determining the water status of leaves.

Index	Formula	Indicators (for)	References
SR	R_{900}/R_{970}	PWC	15
	R_{1300}/R_{1450}	GWC	48
NDWI	$(R_{860} - R_{1240})/(R_{860} + R_{1240})$	EWT	7
NDWI	$(R_{860} - R_{1640})/(R_{860} + R_{1640})$	EWT	49
	$(R_{850} - R_{2218})/(R_{850} - R_{1928})$	EWT and GWC	21
	$(R_{850} - R_{1788})/(R_{850} - R_{1928})$	EWT and GWC	21
Index of moisture stress	R_{1600}/R_{820}	EWT	50
WI using an SRSRWI	R_{860}/R_{1240}	WI	51
Normalized difference WI centered at 1640 nm (NDWI ₁₆₄₀)	$(R_{858} - R_{1640})/(R_{858} + R_{1640})$	WI	49
Normalized difference WI centered at 2130 nm (NDWI ₂₁₃₀)	$(R_{858} - R_{2130})/(R_{858} + R_{2130})$	WI	49

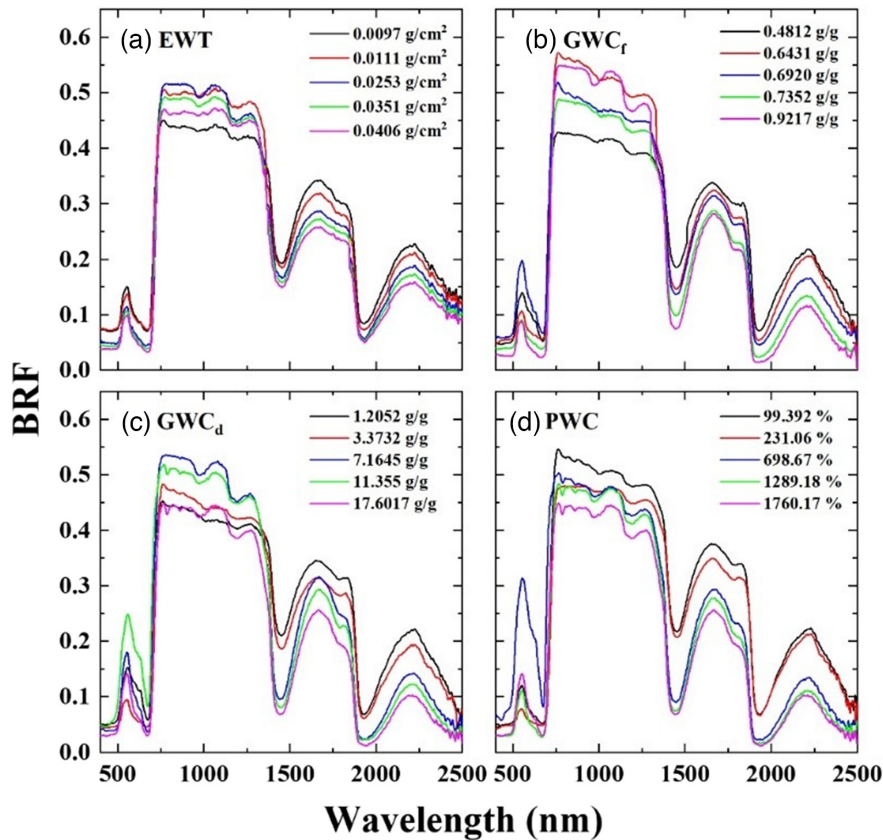


Fig. 2 (a)–(d) Leaves BRF at nadir direction with variables EWT, GWC, and PWC.

2.5 Leaf Reflection Factors: Spectral Properties and Distribution

The spectral reflectance factors with multiple indicators at the nadir view zenith angle are shown in Fig. 2. The considerable absorption of leaf water at wavelengths greater than 1250 nm resulted in the spectral BRF of leaves being constrained as the different water indices shown in the nadir direction in NIR and SWIR wavelengths.³⁸ Various spectral indices are associated with these spectral properties to measure the water content. When the reflectance factor is considered, it can be used to understand the reflection attribute of leaves from various species.

3 Results

3.1 Statistical Analysis

A collection of 277 leaf samples from 10 different species was analyzed to determine the best hyperspectral index for calculating leaf water content. To assist in finding unique indices, several statistical tests were performed on data sets. The best indices were then chosen, and their robustness was verified and validated. First, some basic statistics were applied to the calibration dataset, as shown in Tables 2 and 3. Equations (2)–(5) have been used to calculate the results in Table 2.

Additionally, the regression approach expands to both linear and nonlinear regression. The procedures described were applied to all possible wavelength combinations, and an iterative approach resulted in a wavelength interval of 5 nm.^{28,38} The parameters of published indices were selected using the maximum coefficient of determination (R^2), and the least root mean square error (RMSE). The principal objective was to identify indices with minimum RMSE and the highest R^2 values.

Table 2 The statistics provided below were utilized to calculate the EWT, GWC, and PWC of the samples used.

Name (sample size = 277)		EWT (g/cm ²)	GWC _F (g/g)	GWC _D (g/g)	PWC (%)
<i>Prunus padus L.</i>	Min	0.005	0.451	0.821	82.189
	Max	0.009	0.596	1.480	148.042
	Mean	0.007	0.525	1.120	112.044
<i>Swida alba Opiz</i>	Min	0.006	0.560	1.273	127.384
	Max	0.012	0.706	2.411	241.101
	Mean	0.009	0.645	1.855	185.517
<i>Acer saccharum Marsh</i>	Min	0.005	0.586	1.415	141.583
	Max	0.011	0.791	3.806	380.665
	Mean	0.008	0.696	2.420	242.071
<i>Armeniaca vulgaris Lam</i>	Min	0.007	0.534	1.146	114.607
	Max	0.015	0.690	2.233	223.366
	Mean	0.010	0.612	1.612	161.248
<i>Populus L</i>	Min	0.006	0.546	1.207	120.736
	Max	0.014	0.847	5.544	554.417
	Mean	0.010	0.695	2.451	245.167
<i>Epipremnum aureum</i>	Min	0.018	0.874	6.986	698.671
	Max	0.029	0.946	17.60	1760.17
	Mean	0.024	0.912	10.84	1084.36
<i>Schefflera microphylla Merr</i>	Min	0.016	0.718	2.554	255.492
	Max	0.043	0.919	11.45	1145.16
	Mean	0.031	0.845	5.866	586.645
<i>Pachira aquatica</i>	Min	0.007	0.680	2.133	213.306
	Max	0.015	0.883	7.611	761.161
	Mean	0.011	0.812	4.643	464.320
<i>Juglans</i>	Min	0.007	0.616	1.606	160.630
	Max	0.010	0.764	3.251	325.155
	Mean	0.008	0.689	2.305	230.559
<i>Citrus limon (L.) Burm. F.</i>	Min	0.009	0.527	1.118	111.829
	Max	0.018	0.670	2.035	203.504
	Mean	0.014	0.598	1.527	152.718

Table 3 Summary statistics for calibration data ($n = 277$).

	Mean	Range from min to maxi value	Standard error of mean	Standard deviation	Variation coefficient
EWT	0.01591	0.03792	0.0006	0.0098	0.62
GWC _F	0.7325	0.4951	0.0074	0.1231	0.17
GWC _D	3.922	16.78	0.1783	2.967	0.76
PWC	392.2	1678	17.83	296.7	0.76
Leaf area	59.87	165.3	1.797	29.91	0.49

3.2 Outcome of the Published Indices

Selected published indices performance in this study was analyzed individually to assess variation in EWT, PWC, and GWC. These published indices, which include $(R_{860} - R_{1640}) / (R_{860} + R_{1640})$, $(R_{850} - R_{2218}) / (R_{850} - R_{1928})$, $(R_{850} - R_{1788}) / (R_{850} - R_{1928})$, (R_{1600} / R_{820}) and $(R_{858} - R_{1640}) / (R_{858} + R_{1640})$, have good results in terms of EWT with calibration data sets, and no other indicator have a good result with the calibration dataset. The detail for each indicator and the corresponding results has been given in Table 4.

3.3 Newly Identified Leaf Water Status Index

Calibration dataset for EWT, PWC, and GWC was examined using an iteration process for 5-nm interval for linear [Eq. (7)] and nonlinear [Eq. (8)] regression approaches. The regions with the highest R^2 [Eq. (9)] and lowest RMSE value were finally selected based on reflectance spectra. In general, particular bands were strongly correlated with EWT, PWC, GWC_D , and GWC_F , as shown in Tables 5 and 6. The approach used in this was linear and nonlinear regression, respectively. Overall, the newly identified indices have a notable correlation with EWT, whereas PWC and GWC were not as good as EWT.

3.4 Regression Analysis

Linear and nonlinear regressions were executed to develop models, determine the coefficient of determination between different wavelength ranges and water indices, and compare the model's efficiency

$$\text{Linear regression equation } y_i = \beta_0 + \beta_1 x_i, \quad (7)$$

$$\text{Nonlinear regression equation } y = ae^{bx}, \quad (8)$$

$$\text{Coefficient of determination } R^2 = 1 - \frac{\sum_{i=1}^n (y - \hat{y})^2}{\sum_{i=1}^n (y - \bar{y})^2}, \quad (9)$$

where y_i and x_i are dependent and independent variables, respectively. α , β_0 - intercept; b , β_1 - slope; and \hat{y} refers to the estimated values of dependent variables.

The results for both linear and nonlinear models are shown in Figs. 3 and 4. By looking at the coefficient of determination, we can easily analyze the indices.

3.5 Validation Datasets from Different Sources

The leaf optical properties experiment (LOPEX) of the European Commission's Joint Research Center includes 330 leaf samples from 45 diverse plants.⁵² An experiment conducted at the INRA (National Institute for Agricultural Research) in Angers, France in June 2003, where a dataset associating visible/infrared spectra of vegetation elements with physical measurements and biochemical analyses was constructed. Reflectance and transmittance measurements of 275 leaf samples from 43 different species were collected along with associated biochemical and physical measurements.^{28,53}

Additional data from the LOPEX and ANGERS databases were considered to validate the indices provided in this work and determine their generalizability and reliability. As for both the databases reflectance curves with median spectrum have been measured, as shown in Fig. 5. First, EWT, GWC, and PWC were calculated and further expanded to assess R^2 and RMSE for the proposed spectral indices (Table 7).

In the LOPEX dataset, the proposed index exhibits better results in terms of EWT having a strong coefficient of determination with the lowest RMSE (g/cm^2), as shown in Fig. 6.

The above Fig. 6 shows the result for EWT $(R_{1910} - R_{1340}) / (R_{1910} - R_{1125})$ and $(R_{1930} - R_{1425}) / (R_{1930} - R_{1360})$, GWC_F $(R_{1400} - R_{1835}) / (R_{1400} - R_{1505})$ and $(R_{1395} - R_{1825}) / (R_{1395} + R_{1515})$, GWC_D $(R_{1400} - R_{1835}) / (R_{1400} - R_{1505})$ and $(R_{1515} - R_{1825}) / (R_{1515} - R_{1395})$ and PWC $(R_{1495} - R_{1400}) / (R_{1495} - R_{1830})$, and $(R_{1500} - R_{1400}) / (R_{1500} - R_{1830})$.

Table 4 The evaluation of published water indices for EWT, PWC, and GWC using calibration dataset.

Indices	Indicators	R^2	RMSE
R_{900}/R_{970}	EWT	0.6103	0.0062
	PWC	0.2375	259.5
	GWC_F	0.2499	0.1068
	GWC_D	0.2375	2.595
R_{1300}/R_{1450}	EWT	0.7827	0.0045
	PWC	0.3507	239.5
	GWC_F	0.3327	0.101
	GWC_D	0.3507	2.395
$(R_{860} - R_{1240})/(R_{860} + R_{1240})$	EWT	0.4151	0.0075
	PWC	0.0978	282.3
	GWC_F	0.0965	0.1173
	GWC_D	0.0978	2.823
$(R_{860} - R_{1640})/(R_{860} + R_{1640})$	EWT	0.8451	0.0039
	PWC	0.2602	255.6
	GWC_F	0.2313	0.1082
	GWC_D	0.2602	2.556
$(R_{850} - R_{2218})/(R_{850} - R_{1928})$	EWT	0.8256	0.0041
	PWC	0.2705	253.9
	GWC_F	0.1996	0.1104
	GWC_D	0.2705	2.539
$(R_{850} - R_{1788})/(R_{850} - R_{1928})$	EWT	0.9054	0.0030
	PWC	0.3254	244.1
	GWC_F	0.3020	0.1031
	GWC_D	0.3254	2.441
R_{1600}/R_{820}	EWT	0.8356	0.004
	PWC	0.2808	252.1
	GWC_F	0.2324	0.1081
	GWC_D	0.2808	2.521
R_{860}/R_{1240}	EWT	0.4293	0.0074
	PWC	0.0988	282.1
	GWC_F	0.0998	0.117
	GWC_D	0.0988	2.821
$(R_{858} - R_{1640})/(R_{858} + R_{1640})$	EWT	0.8448	0.0039
	PWC	0.2602	255.6
	GWC_F	0.2314	0.1082
	GWC_D	0.2602	2.556
$(R_{858} - R_{2130})/(R_{858} + R_{2130})$	EWT	0.7542	0.0049
	PWC	0.2634	255.1
	GWC_F	0.1870	0.1112
	GWC_D	0.2634	2.551

Table 5 Evaluation of four types of indices using a linear regression approach.

Indicators	Index	R^2	RMSE
EWT	$(R_{1910} - R_{1340}) / (R_{1910} - R_{1125})$	0.969	0.001
PWC	$(R_{1495} - R_{1400}) / (R_{1495} - R_{1830})$	0.863	0.003
GWC_D	$(R_{1400} - R_{1835}) / (R_{1400} - R_{1505})$	0.863	0.003
GWC_F	$(R_{1400} - R_{1835}) / (R_{1400} - R_{1505})$	0.896	0.002

Table 6 Using a nonlinear regression technique, four different types of indices are evaluated.

Indicators	Index	R^2	RMSE
EWT	$(R_{1930} - R_{1425}) / (R_{1930} - R_{1360})$	0.959	0.001
PWC	$(R_{1500} - R_{1400}) / (R_{1500} - R_{1830})$	0.882	0.003
GWC_D	$(R_{1515} - R_{1825}) / (R_{1515} - R_{1395})$	0.882	0.003
GWC_F	$(R_{1395} - R_{1825}) / (R_{1395} + R_{1515})$	0.895	0.002

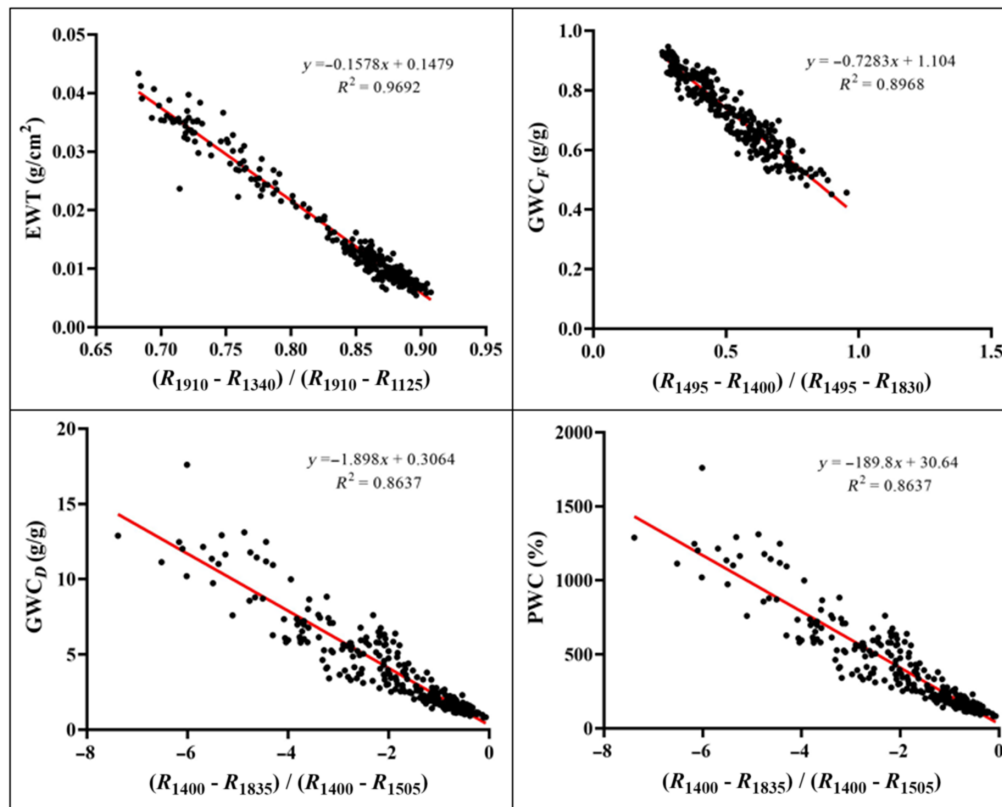


Fig. 3 Utilizing calibration data, linear regression models were used to calculate the coefficient of determination of the selected wavelength and WI (EWT, GWC_F , GWC_D , and PWC).

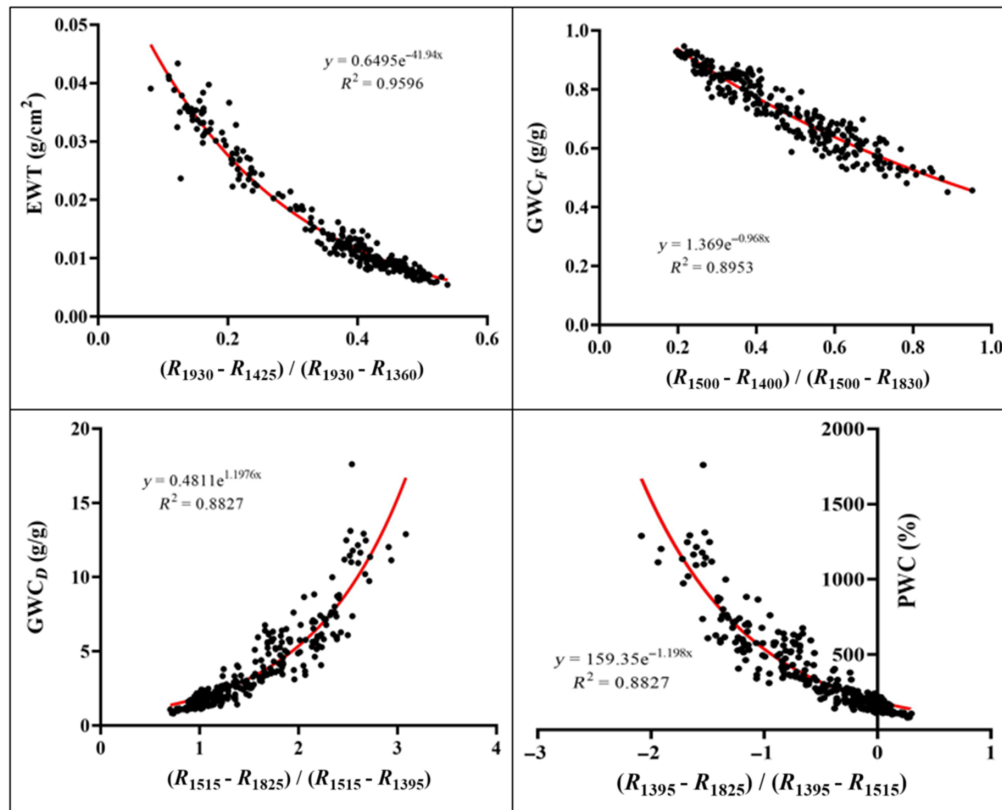


Fig. 4 Nonlinear regression models were used to obtain the coefficient of determination of the selected wavelength and WI using calibration data (EWT, GWC_F, GWC_D, and PWC).

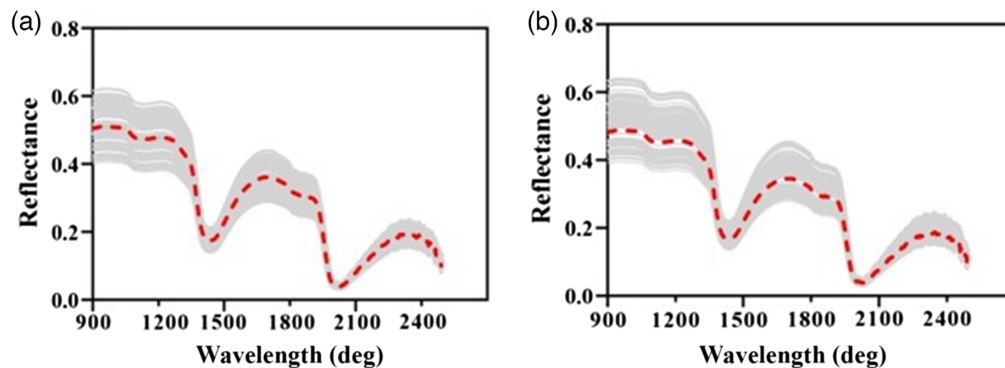


Fig. 5 Reflectance spectrum from validation dataset (a) ANGERS and (b) LOPEX. The median spectrum is shown by the dashed red line.

While in the ANGERS dataset, the indicators were individually compared to the proposed indices. The results were encouraging for EWT, which had the highest R^2 and minimum RMSE values, as shown in Fig. 7.

The Fig. 7 presented the result for EWT $(R_{1910} - R_{1340}) / (R_{1910} - R_{1125})$ and $(R_{1930} - R_{1425}) / (R_{1930} - R_{1360})$, GWC_D $(R_{1400} - R_{1835}) / (R_{1400} - R_{1505})$ and $(R_{1515} - R_{1825}) / (R_{1515} - R_{1395})$ and PWC $(R_{1495} - R_{1400}) / (R_{1495} - R_{1830})$, and $(R_{1500} - R_{1400}) / (R_{1500} - R_{1830})$.

So generally, it is concluded that both the databases, i.e., LOPEX and ANGERS have good correlations with the suggested indices (linear and nonlinear), specifically with EWT. While for the other two indices, such as GWC and PWC, LAI is not involved in measuring water content.

Table 7 Validation datasets to calculate EWT, GWC, and PWC.

	LOPEX	ANGERS
Spectrophotometer	Perkin Elmer Lambda 19	ASD FieldSpec
Estimation	Laboratory	Laboratory
Spectral range	400 to 2500	350 to 2500 (nm)
Sample size	45	43
Mean (g/cm ²)	0.0111	0.0116
Min (g/cm ²)	0.0003	0.0044
Max (g/cm ²)	0.0525	0.0340
References	52	53

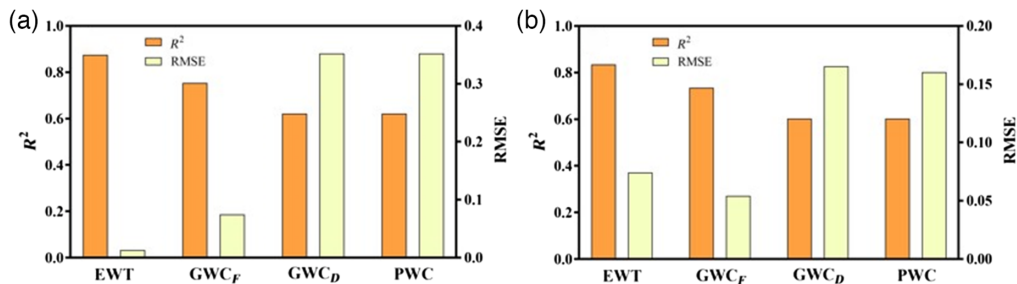


Fig. 6 The validation of results of both linear and nonlinear indices of EWT, GWC_F, GWC_D, and PWC. Based on using the LOPEX database, RMSE is computed based on these models; R^2 is the determination coefficient, where panels (a) and (b) refer to linear and nonlinear regression indices, respectively.

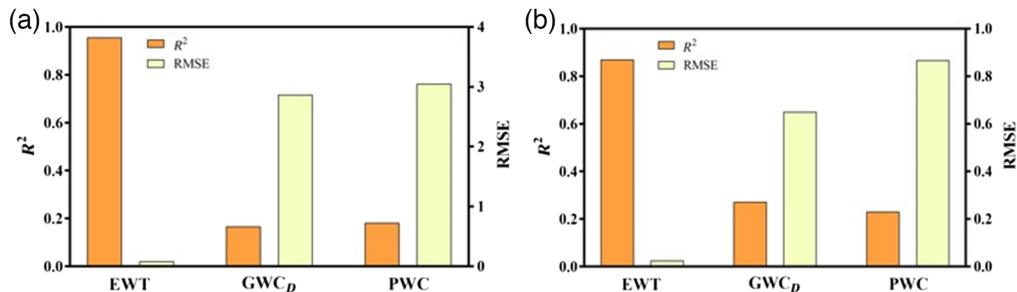


Fig. 7 The validation of results of the EWT, GWC, and PWC based on using the ANGERS database. RMSE is calculated based on these models and R^2 is the determination coefficient. Panels (a) and (b) refer to linear and nonlinear regression indices, respectively.

3.6 Best Indicators for Defining the Status of Leaf Water

Ratio of modified difference, normalized difference index, double difference ($R1 - R2/R1 - R3$), and simple ratios (SR) are the most commonly used criteria for evaluating leaf water indices. These criteria typically disrupt standard water-absorbing indices, such as water index (WI), normalized differential water index (NDWI), and water index using a simple ratio (SRWI), because they vary and use different wavelengths. Our findings also show that the combination of the ($R1-R2$) and ($R1-R3$) bands significantly impacts the status of leaf water. In this study,

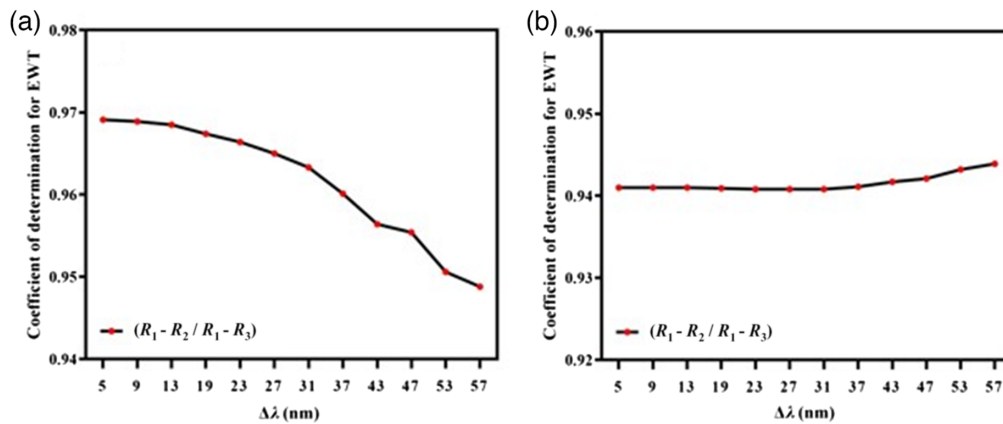


Fig. 8 From calibration dataset: suggested bandwidth index for EWT with reliable stability showing both (a) linear and (b) nonlinear indices.

the linear regression model $(R_{1910} - R_{1340}) / (R_{1910} - R_{1125})$ having $R^2 = 0.9692$ and $\text{RMSE} = 0.0017$ (g/cm^2) while the nonlinear regression model $(R_{1930} - R_{1425}) / (R_{1930} - R_{1360})$ having $R^2 = 0.9596$ and $\text{RMSE} = 0.0019$ (g/cm^2) shows good results as compared to the already published indices. Therefore, the recommended indices are more dependable and persistent in calculating leaf water content for the plants species used in this study.

The results have been further verified by LOPEX and ANGERS datasets; as we can see in Fig. 7, both the suggested indices have performed well in terms of R^2 and RMSE, which further strengthens the results on the proposed linear and nonlinear indices. Figure 7 indicates that EWT, with LOPEX and ANGERS, has come up with better results than the other water indicators, such as GWT and PWC.⁵⁴ Both, the indices have shown reliable results with calibration data set, but to make these indices more generalized and could be used for any type of plant leaf that's why we have to check the accuracy and the reliability of the proposed indices with already published and worldwide used databases, such as LOPEX and ANGERS and while looking at the results, as shown in Fig. 7, we can see that the indices proposed in this study are reliable and accurate.

4 Discussion

4.1 Stability of the Index Suggested

The proposed EWT linear and nonlinear indices were tested with odd combinations until 57 nm in both a forward and backward manner within the calibration dataset. The combination of the proposed indices has been made with the difference of odd numbers (to take the average), such as 5, 9, and 13 nm, until 57 nm and they showed stability and a strong determination coefficient on both aspects, indicating their correctness and dependability as shown in Fig. 8. Theoretically, a valid and reliable index should be assessed for calibration on numerous datasets with varying random percentages and to keep high stability under different wavelength resolution.^{38,55} Newly proposed indices have the potential to be expanded to enormous sizes and would satisfy future applications due to their intensity and dependability.³⁸

4.2 Leaf Properties Based on Individual Wavelength

We have checked the individual wavelength and their correlation coefficients. In the single band, the correlation coefficient is relatively low with the calibration dataset. But these individual bands play a crucial role in estimating leaf water content because they cover the sensitive region where water can be traced. The main theme of doing this is to show how they respond separately, and when it came to bands combination, they have shown good results. As a result, we used a technique that included specified steps to examine how each band of the indices related to reflectance, as shown in Fig. 9.

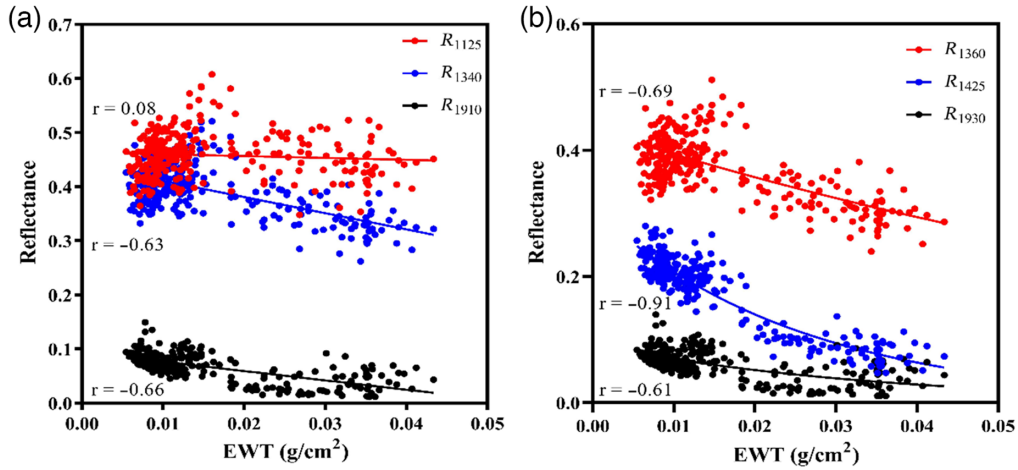


Fig. 9 Relationship between EWT and reflectance from calibration data set at (a) linear (bands): R_{1125} , R_{1340} , and R_{1910} (nm) and (b) non-linear (bands): R_{1360} , R_{1425} , and R_{1930} (nm). Power curves of the form best represented the relationships as $y = ax^{-b}$. Correlation coefficients (r) are shown.

The mean spectra of leaves for various EWT ranges are illustrated in Fig. 10. At 1350 to 1580 nm, leaves with high EWT and other indicators show comparatively low reflectance. The spectral region of the reflectance spectrum is primarily influenced by pigment absorption (mostly by chlorophyll molecules).^{56,57} Increased relative reflectance at wavelengths between 1400–1580 nm resulted from the dehydration of leaves, affecting their optical characteristics. However, numerous published research documents erratic changes in leaf reflectance during dehydration, such as an overall rise, a decrease, and no significant fluctuations in reflectance.^{56,58} After using the first derivative of relative reflectance, these outcomes were more obvious as shown in Fig. 10(b). The trend of the Pearson’s correlation coefficients (r_P) in the relationship between the EWT and wavelength-dependent relative reflectance values shown in Fig. 10(c).^{18,34} While Fig. 10(d) demonstrates how r_P has changed over time in the relationship between the wavelength dependent first derivative of the relative reflectance values and EWT.

As Fig. 11 demonstrates that the indices’ values are restricted to the ranges of 0.6 to 1.0 for LOPEX and 0.001 to 0.04 for ANGERS (horizontal axis). Leaf samples were utilized to evaluate

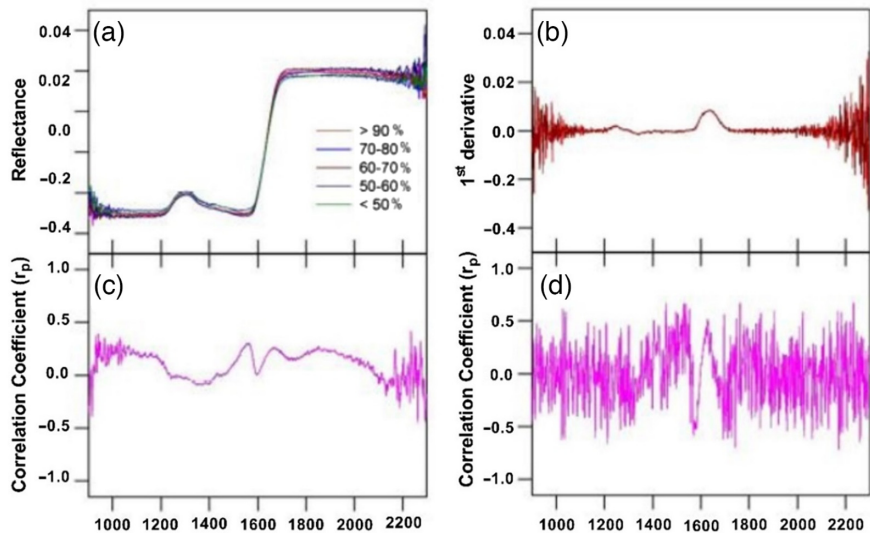


Fig. 10 (a) Reflectance spectral signatures, (b) first derivative for reflectance, (c) EWT correlation coefficient (r_P) and reflectance spectra correlation, and (d) first derivative of reflectance.

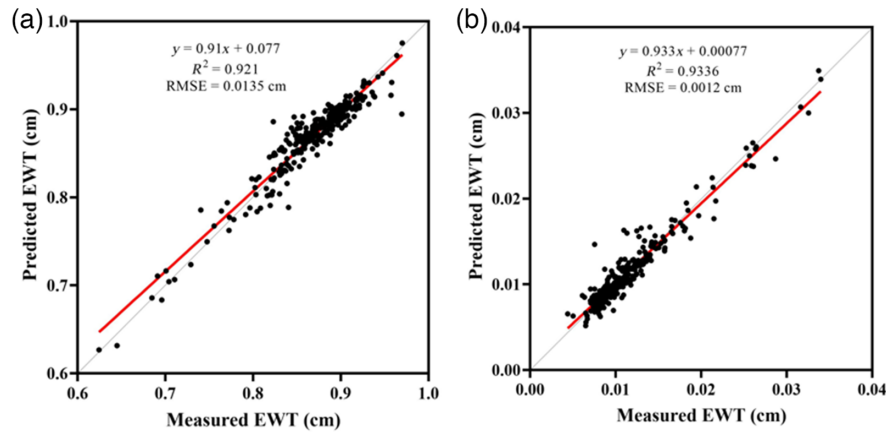


Fig. 11 The results of validation of EWT based on using the (a) LOPEX and (b) ANGERS databases. RMSE is computed based on the EWT model and R^2 is the coefficient of determination.

the model. The relative RMSE was calculated in relation to the mean measured values. Overall, it is evident that the model's predicted values and the measured values exhibit a strong linear positive connection. Most of the existing research on the association between the water content of leaves and their ability to reflect light (particularly EWT) is restricted to several unique species and specific wavelengths. However, in our study, we try not to keep ourselves to specific species; as a result, the method applies to any species for EWT calculation.

Due to changes in water indices and interior leaf structure, the spectral reflectance fluctuates slightly, mainly in the infrared and NIR. This study examines whether a water sensitivity index can accurately estimate the EWT of different plant species.

4.3 Advantages of the Proposed Indices

Nowadays, most EWT indices are calculated using measurements of the reflectance factors of leaves obtained with an integrating sphere, a spectrometer equipped with a leaf clip, or a spectrometer positioned close to the nadir direction.⁵⁰ Although it has not received much attention from academics seeking to estimate EWT, the specular reflection off the leaf surface in these directions has little impact on spectral reflection measurements. In a variety of illumination-viewing geometries over a wide range of species, the newly suggested index can reduce the specular reflection brought on by the leaf surface. Compared to other existing indices in this study, this enables these indices to have the best relationship with EWT and the lowest sensitivity to reflectance variables.

The proposed indices also have the advantage of being adaptable to additional observed and simulated datasets containing reflected signals from other plant species in various geographic locations or regions under various measurement conditions. The reflectance factors of leaves take into account reflection values that are equivalent to those measured by leaf clip or integrating sphere, as well as reflectance factors that are dominated by specular reflection from the leaf surface, which result in the expected phenomena.

5 Conclusion

This study evaluated how effectively several indices performed while estimating EWT, PWC, GWC_F , and GWC_D . In estimating EWT for different plant species, most spectral indices based on the theory of water absorption performed surprisingly well, having the highest R^2 and the lowest RMSE value. Since PWC and GWC did not perform well, it is inferred that EWT is the water-sensitive spectral indices. The final EWT linear and nonlinear indices are $(R_{1910} - R_{1340}) / (R_{1910} - R_{1125})$ and $(R_{1930} - R_{1425}) / (R_{1930} - R_{1360})$, respectively.

The Datt type of index, $(R_1 - R_2) / (R_1 - R_3)$, is a sensitive indicator for estimating plant species' leaf water content since it is based on the ratio of differences of three wavelengths.

This index cannot only estimate water content with high accuracy but also estimate leaf water content with reflection with the same precision as one direction. In this study, we looked into the effectiveness of specific hyperspectral indices in determining EWT, PWC, and GWC. As a result, it is concluded that EWT measured the water-sensitive spectral indices instead of PWC and GWC.

The Datt type of index, the ratio of reflectance differences, can be used to reduce specular reflection and then estimate leaf water content with quite consistent and high accuracy for the plant species in this research. Because specular reflection alters the association of spectral indices with leaf water content, as a physical optical characteristic of a leaf, it is considered “noise” in assessing leaf water content.

These indices can be used for reflected signals from various plant species in various locations or regions and under various measurement settings. This is because leaf reflectance factors contain reflectance factors primarily caused by specular reflection off the leaf surface in addition to reflection values similar to those obtained using a leaf clip or an integrating sphere. More research is needed to see if the Datt type can be used to remotely estimate the leaf water content of other plant species with varied leaf surfaces.

Acknowledgments

This study was jointly financed by the Key R & D and Transformation Program of Qinghai Province (Grant No. 2020-SF-C37) and the National Key R & D Program of China (Grant No. 2016YFA0602302). The authors declare no conflict of interest.

References

1. C. Quemada et al., “Remote sensing for plant water content monitoring: a review,” *Remote Sens.* **13**, 2088 (2021).
2. Q. Wang and J. Jin, “Hyperspectral remote sensing of plant water status and plant water use under drought stress,” in *Green Science and Technology*, E. Y. Park et al., Eds., CRC Press, Boca Raton, Florida (2019).
3. J. Féret et al., “Estimating leaf mass per area and equivalent water thickness based on leaf optical properties: potential and limitations of physical modeling and machine learning,” *Remote Sens. Environ.* **231**, 110959 (2018).
4. S. M. De Jong, E. A. Addink, and J. C. Doelman, “Detecting leaf-water content in Mediterranean trees using high-resolution spectrometry,” *Int. J. Appl. Earth Obs. Geoinf.* **27**, 128–136 (2014).
5. E. Neinavaz et al., “Agricultural and forest meteorology retrieving vegetation canopy water content from hyperspectral thermal measurements,” *Agric. For. Meteorol.* **247**, 365–375 (2017).
6. P. S. Thenkabail et al., “Hyperspectral remote sensing of vegetation and agricultural crops,” *Photogramm. Eng. Remote Sens.* **80**(8), 695–723 (2014).
7. B. C. Gao, “NDWI - a normalized difference water index for remote sensing of vegetation liquid water from space,” *Remote Sens. Environ.* **58**, 257–266 (1996).
8. P. J. Zarco-Tejada, C. A. Rueda, and S. L. Ustin, “Water content estimation in vegetation with MODIS reflectance data and model inversion methods,” *Remote Sens. Environ.* **85**, 109–124 (2003).
9. X. Wang et al., “Determining the canopy water stress for spring wheat using canopy hyperspectral reflectance data in loess plateau semiarid regions,” *Int. J. Rapid Commun.* **48**, 492–498 (2015).
10. P. Bowyer and F. M. Danson, “Sensitivity of spectral reflectance to variation in live fuel moisture content at leaf and canopy level,” *Remote Sens. Environ.* **92**, 297–308 (2004).
11. F. M. Danson and P. Bowyer, “Estimating live fuel moisture content from remotely sensed reflectance,” *Remote Sens. Environ.* **92**, 309–321 (2004).
12. P. Ceccato et al., “Detecting vegetation leaf water content using reflectance in the optical domain,” *Remote Sens. Environ.* **77**, 22–33 (2001).

13. F. M. Danson et al., "High-spectral resolution data for determining leaf water content," *Int. J. Remote Sens.* **13**, 461–470 (1992).
14. L. Liu, S. Zhang, and B. Zhang, "Evaluation of hyperspectral indices for retrieval of canopy equivalent water thickness and gravimetric water content," *Int. J. Remote Sens.* **37**, 3384–3399 (2016).
15. J. Penuelas et al., "Estimation of plant water concentration by the reflectance Water Index WI (R900/R970)," *Int. J. Remote Sens.* **18**, 2869–2875 (1997).
16. Z. Satti et al., "Effects of climate change on vegetation and snow cover area in Gilgit Baltistan using MODIS data," *Environ. Sci. Pollut. Res.* **30**, 19149–19166 (2022).
17. M. Naveed et al., "Analyzing the impact of climate change on cotton yield using spatial analysis and statistical modeling in the Indus River Basin, Pakistan," *Ann. Agric. Crop Sci.* **6**, 1089 (2021).
18. R. Colombo et al., "Estimation of leaf and canopy water content in poplar plantations by means of hyperspectral indices and inverse modeling," *Remote Sens. Environ.* **112**, 1820–1834 (2008).
19. Q. Yi et al., "Leaf and canopy water content estimation in cotton using hyperspectral indices and radiative transfer models," *Int. J. Appl. Earth Observ. Geoinf.* **33**, 67–75 (2014).
20. J. Penuelas et al., "The reflectance at the 950-970 nm region as an indicator of plant water status," *Int. J. Remote Sens.* **14**, 1887–1905 (1993).
21. B. Datt, "Remote sensing of water content in Eucalyptus leaves," *Aust. J. Bot.* **47**(6), 909–923 (1999).
22. Q. Yi et al., "Estimation of leaf water content in cotton by means of hyperspectral indices," *Comput. Electron. Agric.* **90**, 144–151 (2013).
23. C. J. Tucker, "Remote sensing of leaf water content in the near infrared," *Remote Sens. Environ.* **10**, 23–32 (1980).
24. E. Garnier and G. Laurent, "Leaf anatomy, specific mass and water content in congeneric annual and perennial grass species," *New Phytol.* **128**(4), 725–736 (1994).
25. E. B. Knipling, "Physical and physiological basis for the reflectance of visible and near-infrared radiation from vegetation," *Remote Sens. Environ.* **1**(3), 155–159 (1970).
26. S. W. Running and R. R. Nemani, "Regional hydrologic and carbon balance responses of forests resulting from potential climate change," *Clim. Change* **19**, 349–368 (1991).
27. L. Zhang et al., "Monitoring the leaf water content and specific leaf weight of cotton (*Gossypium hirsutum* L.) in saline soil using leaf spectral reflectance," *Eur. J. Agron.* **41**, 103–117 (2012).
28. Y. Qm and W. Zhang, "Estimation of leaf water content of different leaves from different species using hyperspectral reflectance data," *Ann. Agric. Sci.* **7**, 1111–2022 (2022).
29. G. A. Carter, "Primary and secondary effects on water content on the spectral reflectance of leaves," *Am. J. Bot.* **78**(7), 916–924 (1991).
30. Z. Wang et al., "Shrinkage and fragmentation of grasslands in the West Songnen Plain, China," *Agric. Ecosyst. Environ.* **129**, 315–324 (2009).
31. J. Peñuelas et al., "Reflectance indices associated with physiological changes in nitrogen- and water-limited sunflower leaves," *Remote Sens. Environ.* **48**, 135–146 (1994).
32. W. Li et al., "Recent changes in global photosynthesis and terrestrial ecosystem respiration constrained from multiple observations," *Geophys. Res. Lett.* **45**(2), 1058–1068 (2018).
33. A. Elsherif et al., "Three dimensional mapping of forest canopy equivalent water thickness using dual-wavelength terrestrial laser scanning," *Agric. For. Meteorol.* **276–277**, 107627 (2019).
34. M. Fang et al., "A new spectral similarity water index for the estimation of leaf water content from hyperspectral data of leaves," *Remote Sens. Environ.* **196**, 13–27 (2017).
35. T. Koike, "A method for measuring photosynthesis with detached parts of deciduous broad-leaved trees in Hokkaido," *J. Jpn. For. Soc.* **68**(10), 425–428 (1986).
36. A. D. Richardson and G. P. Berlyn, "Changes in foliar spectral reflectance and chlorophyll fluorescence of four temperate species following branch cutting," *Tree Physiol.* **22**, 499–506 (2002).
37. S. Foley et al., "Foliar spectral properties following leaf clipping and implications for handling techniques," *Remote Sens. Environ.* **103**(3), 265–275 (2006).

38. Z. Cao, Q. Wang, and C. Zheng, “Best hyperspectral indices for tracing leaf water status as determined from leaf dehydration experiments,” *Ecol. Indic.* **54**, 96–107 (2015).
39. A. Gitelson and M. N. Merzlyak, “Spectral reflectance changes associated with autumn senescence of *Aesculus hippocastanum* L. and *Acer platanoides* L. leaves. Spectral features and relation to chlorophyll estimation,” *J. Plant Physiol.* **143**(3), 286–292 (1994).
40. F. Verlaet et al., “Relationships between leaf chlorophyll content and spectral reflectance and algorithms for non-destructive chlorophyll assessment in higher plant leaves,” *J. Plant Physiol.* **160**, 271–282 (2003).
41. Z. Q. Sun et al., “Semi-automatic laboratory goniospectrometer system for performing multi-angular reflectance and polarization measurements for natural surfaces,” *Rev. Sci. Instrum.* **85**, 014503 (2014).
42. Z. Sun et al., “Optical properties of reflected light from leaves: a case study from one species,” *IEEE Trans. Geosci. Remote Sens.* **57**(7), 4388–4406 (2019).
43. J. Sun et al., “Wavelength selection of the multispectral lidar system for estimating leaf chlorophyll and water contents through the PROSPECT model,” *Agric. For. Meteorol.* **266**, 43–52 (2019).
44. Z. Sun et al., “Photopolarimetric properties of leaf and vegetation covers over a wide range of measurement directions,” *J. Quantum Spectrosc. Radiat. Transf.* **206**, 273–285 (2018).
45. G. Schaepman-strub et al., “Reflectance quantities in optical remote sensing — definitions and case studies,” *Remote Sens. Environ.* **103**, 27–42 (2006).
46. S. Jacquemoud et al., “Estimating leaf biochemistry using the PROSPECT leaf optical properties model,” *Remote Sens. Environ.* **56**(3), 194–202 (1996).
47. G. Le Maire et al., “Calibration and validation of hyperspectral indices for the estimation of broadleaved forest leaf chlorophyll content, leaf mass per area, leaf area index and leaf canopy biomass,” *Remote Sens. Environ.* **112**, 3846–3864 (2008).
48. H. D. Seelig et al., “Extraneous variables and their influence on reflectance-based measurements of leaf water content,” *Irrig. Sci.* **26**, 407–414 (2008).
49. D. Chen, J. Huang, and T. J. Jackson, “Vegetation water content estimation for corn and soybeans using spectral indices derived from MODIS near- and short-wave infrared bands,” *Remote Sens. Environ.* **98**, 225–236 (2005).
50. E. R. Hunt and B. N. Rock, “Detection of changes in leaf water content using near- and middle-infrared reflectances,” *Remote Sens. Environ.* **30**, 43–54 (1989).
51. P. J. Zarco-Tejada and S. L. Ustin, “Modeling canopy water content for carbon estimates from MODIS data at land EOS validation sites,” in *Proc. Int. Geosci. and Remote Sens. Symp. (IGARSS)* (2001).
52. B. Hosgood et al., “Leaf optical properties experiment 93 (LOPEX93),” Report EUR, 16095 (1995).
53. J. Feret et al., “PROSPECT-4 and 5: advances in the leaf optical properties model separating photosynthetic pigments,” *Remote Sens. Environ.* **112**, 3030–3043 (2008).
54. X. Li et al., “A multi-angular invariant spectral index for the estimation of leaf water content across a wide range of plant species in different growth stages,” *Remote Sens. Environ.* **253**, 112230 (2021).
55. Z. Gao et al., “The responses of vegetation water content (EWT) and assessment of drought monitoring along a coastal region using remote sensing,” *GISci. Remote Sens.* **51**, 37–41 (2014).
56. M. Kovar et al., “Evaluation of hyperspectral reflectance parameters to assess the leafwater content in soybean,” *Water* **11**, 1–12 (2019).
57. M. Naveed and H. S. He, “Cotton cultivated area detection and yield monitoring combining remote sensing with field data in lower Indus River basin, Pakistan,” *Environ. Monit. Assess.* **195**, 401 (2023).
58. H. D. Seelig et al., “The assessment of leaf water content using leaf reflectance ratios in the visible, near-, and short-wave-infrared,” *Int. J. Remote Sens.* **29**, 3701–3713 (2008).

Qazi Muhammad Yasir received his MS degree in cartography and geography information system from Northeast Normal University, Changchun, China. Currently, he is pursuing his doctoral degree in remote sensing and geography information system mainly focusing on remote

sensing and GIS at Mary Immaculate College, University of Limerick Ireland. His research interests include hyperspectral data analysis, spatial data analysis, geo statistical data analysis, hazard mapping, site selection, and machine learning.

Zhijie Zhang is pursuing his PhD in geography mainly focusing on remote sensing and GIS studies in global change at the University of Connecticut, Connecticut, United States. From 2016 to 2017, he was a research student in WINLAB, Rutgers and involved in 2 IOT sensor network projects. From 2018 until now, he has been a research assistant in geography department, University of Connecticut, mainly engaging in applying deep learning methods in remote sensing, hydrology, and disaster studies.

Jiakui Tang (PhD) is working as an associate professor at the College of Resources and Environment, University of Chinese Academy of Sciences. His research interests include environment remote sensing remote sensing image processing, aerosol remote sensing, and cloud computing for spatial information processing.

Muhammad Naveed received his MS degree in statistics from Islamia University Bahawalpur, Pakistan. Currently, he is pursuing his doctoral degree in remote sensing and geography information system at Northeast Normal University, China. His research interests include geo statistical analysis, spatial data analysis, crop and drought monitoring, hazard mapping, and machine learning.

Zahid Jahangir received his master's degree in cartography and geographical information engineering from State Key Laboratory of Information Engineering in Surveying, Mapping and Remote Sensing, Wuhan University, Wuhan, China. Currently, he is pursuing his PhD in cartography and geographical information engineering mainly focusing on remote sensing and GIS integration for data extraction and improvement for multiple applications, such as land surface temperature downscaling, agriculture, site selection, and disaster management.